

Abrasion Resistant thin Partially Stabilised Zirconia Coatings by Sol-gel Dip-coating

H. Ivanković, J. Macan*, M. Ivanković, and K. Grilec**

Faculty of Chemical Engineering and Technology, University of Zagreb, Marulićev trg 19, p.p. 177, 10001 Zagreb, Croatia

**Faculty of Mechanical Engineering and Naval Architecture, University of Zagreb, Ivana Lučića 5, p.p.102, 10002 Zagreb, Croatia

Original scientific paper

Received: January 7, 2004

Accepted: December 15, 2004

Thin partially stabilised zirconia coatings were prepared by dip-coating from sols. $Zr(O-nC_4H_9)_4$ was used as zirconia precursor in sol-gel synthesis, making use of yttria to stabilise the high-temperature zirconia modifications. The effect of synthesis parameters for sol, such as molar ratio of $Zr(O-nC_4H_9)_4$, 2,4-pentadione, water and nitric acid on the stability of ZrO_2 sols, was determined. The gelling time was largely extended from 0 to 4 200 h by increasing the molar ratio of 2,4-pentadione to $Zr(O-nC_4H_9)_4$ from 0 to 0.8. The acid displayed a marked catalytic and, combined with 2,4-pentadione, synergistic effects on the hydrolysis rate of $Zr(O-nC_4H_9)_4$. Crystallographic analysis showed that only tetragonal zirconia crystallized at 673 K, and that it remains stable until ~ 1173 K. Optical microscopy of thin zirconia coatings showed that increased firing temperature facilitated the grain growth of zirconia. The mechanical properties (microhardness and abrasion resistance) of the coating-substrate system also increased with increasing the firing temperature and viscosity of the coating solution.

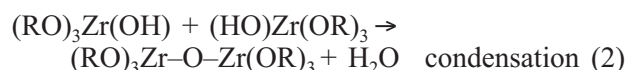
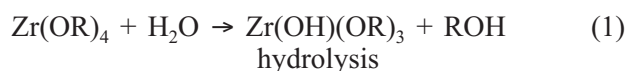
Key-words:

Sol-gel, dip-coating, zirconia, thin coatings, tribology

Introduction

Thin ceramic coatings on steels have proven to be efficient in improving the tribologic and corrosion resistance of the substrates, and zirconia, ZrO_2 , is often used for this purpose.^{1–10} The monoclinic (m) form of zirconia is stable until 1443 K, when it transforms into tetragonal (t) form.¹¹ Since the m \rightarrow t transformation entails a significant change in volume (3–5%), which can cause the cracking of films, the tetragonal or cubic form of zirconia is stabilised by addition of various dopants: MgO, CaO, Y_2O_3 , CeO_2 , Yb_2O_3 , NiO.¹² Because of its high hardness, toughness and corrosion resistance, a mixture of cubic and tetragonal or monoclinic zirconia, or partially stabilized zirconia (PSZ), is an especially attractive coating material.^{13–15} Sol-gel procedure, as a novel method for preparing PSZ coating, is gaining popularity due to its simplicity. It allows preparation of very pure and homogenous coatings at low temperatures, at the same time allowing the control over the final microstructure.

Decisive factor for the PSZ coating quality is the successful control of reactions of hydrolysis and condensation of zirconium alkoxide during the sol-gel process. These reactions can be presented in a simplified manner as follows:



Reaction of hydrolysis is considerably faster than the condensation reaction, which results in undesirable precipitation of zirconium hydroxide. This can be prevented by complexing of zirconium alkoxide with organic ligands, such as 2,4-pentadione,^{2,16} organic acids^{1,5} and glycols.¹⁷

The goal of this work was to investigate the conditions for preparing a stable zirconia sol for PSZ coatings. The influence of synthesis parameters on the rate of hydrolysis and condensation, and hence on zirconia sol stability, was monitored. The influence of thermal treatment on the final properties of thin PSZ coatings was determined by crystallographic analysis, optical microscopy and mechanical measurements.

Experimental

Preparation and stabilisation of zirconia sols

The sols were prepared by dissolving $Zr(O-nC_4H_9)_4$ and 2,4-pentadione in 2-propanol. The complexing agent 2,4-pentadione was added to $Zr(O-nC_4H_9)_4$ in molar ratio 0–0.8. Partial stabilisa-

*Corresponding author: tel. ++385-1-4597-226; fax. ++385-1-4597-250; e-mail: jmacan@pierre.fkit.hr

Table 1 – Influence of the composition on gelling time and appearance of zirconia sols

Sol No.	Molar ratio, r/mol				Gelling time* t/h	Appearance
	Zr(O–nC ₄ H ₉) ₄	2,4-pentadione	water	HNO ₃		
1	1	0.0	2	0.00	0	white precipitate
2	1	0.4	2	0.00	0	white precipitate
3	1	0.5	2	0.00	0	yellow gel
4	1	0.6	2	0.00	12	transparent yellow sol
5	1	0.6	2	0.05	8	transparent yellow sol
6	1	0.6	2	0.20	6	transparent yellow sol
7	1	0.7	2	0.00	1485	transparent yellow sol
8	1	0.7	2	0.05	525	transparent yellow sol
9	1	0.7	2	0.20	122	transparent yellow sol
10	1	0.8	2	0.00	4200	transparent yellow sol
11	1	0.8	2	0.05	2775	transparent yellow sol
12	1	0.8	2	0.20	145	transparent yellow sol

*Time when the ball in the Hoppler viscometer was not able to fall freely through the tube (the ball started “to dance”)

tion of the final zirconia coating was achieved by addition of $w = 3\%$ of yttria, in the form of yttrium acetate hydrate, $\text{Y}(\text{CH}_3\text{COO})_3 \cdot 4\text{H}_2\text{O}$. Reactions of hydrolysis and condensation were initiated by adding 2 moles of water per mole of $\text{Zr}(\text{O}-\text{nC}_4\text{H}_9)_4$, or by aqueous solution of nitric acid containing the same amount of water. Molar ratio of HNO_3 to $\text{Zr}(\text{O}-\text{nC}_4\text{H}_9)_4$ in final sols was thus 0, 0.05 and 0.2, respectively. Designations of all sols, as well as their compositions and gelling times, are given in Table 1. The stability of prepared sols and their gelling kinetics were monitored by the Höppler falling ball viscosimeter, with a tube of 10° inclination, at the constant temperature of 293 K.

Characterisation of crystallisation behaviour

Final gels were dried at 378 K for 24 h, ground in an agate mortar, and characterised by simultaneous differential scanning calorimetry/thermogravimetric analysis (DSC/TGA) on a Netzsch thermoanalyzer STA 409. Samples were heated from room temperature to 1473 K at a rate of temperature change $T = 10 \text{ K min}^{-1}$ in a synthetic air flow. Influence of the firing temperature on the phase composition of zirconia powders was examined by X-ray diffraction analysis (XRD) of the samples fired for 2 h on different temperatures, on Phillips PW 1010 instrument making use of $\text{CuK}\alpha$ radiation.

Coating procedure and characterisation

Stainless steel DIN 1.4923, grade X22CrMoV121, was used as a substrate for the application of zirconia coatings. The substrate surface was finely pol-

ished. The substrates ($70 \times 18 \times 8 \text{ mm}$ plates) were dipped in a zirconia sol (the sol no. 8 in Table 1) by means of a home-made apparatus and drawn at a constant rate of 0.7 mm s^{-1} . The dynamic viscosity, η , of the fresh sol was 4.0 mPa s . The coated substrate was dried for an hour at room temperature, and then at 378 K for 24 h, and finally fired in a furnace at 673 K, 773 K, 873 K and 973 K, over the 2 h period. The furnace was heated up to the final temperature with the rate of 1 K min^{-1} . The procedure of dipping, drying and firing was repeated three times. To determine the influence of sol viscosity, substrates were also dipped in aged sols (the dynamic viscosities were 5.4, 6.1 and 8.1 mPa s), with identical further treatment at 673 K.

Morphology of the coatings was observed by optical microscope Olympus BH-2 with maximum magnification of 1000:1.

Microhardness was measured using Zwick hardness tester by Knoop method¹⁸, with a rhombic-based pyramidal diamond indenter. The indenter is pressed into the sample by an accurately controlled test force. Test forces applied are listed in Table 2. (In the designated tests the number following “HK” means the test load in kg). The force

Table 2 – Test forces applied in hardness testing by Knoop method

Designation	HK0.01	HK0.02	HK0.03	HK0.05	HK0.1	HK0.2
Force F/N	0.0981	0.1961	0.2942	0.4903	0.9807	1.9613

is maintained for a dwell time (10 s) and the indenter is removed leaving an elongated diamond shaped indent in the sample. The dimension of the indent is determined optically by measuring the longest diagonal of the diamond shaped indent. To calculate the Knoop hardness, HK, the following formula is used:

$$HK = 1.451 \frac{F}{d^2}$$

where F is the test force in N and d is the length of the longest diagonal in mm.

The abrasion resistance was measured by contact with a rotating abrasive ring. The abrasive used was SiC paper (average grain diameter $5 \mu\text{m}$), with loading force of 1.5 N and rotation speed of 30 min^{-1} .

Results and discussion

Zirconia sols

In order to control the rate of hydrolysis and condensation of $\text{Zr}(\text{O}-n\text{C}_4\text{H}_9)_4$, the influence of 2,4-pentadione and acid on the gelling kinetics was investigated. The results are shown in Table 1, and in Figures 1 and 2. In sols where 2,4-pentadione is not present, or is present in the ratio of 0.4 or less, white zirconium hydroxide precipitates suddenly.

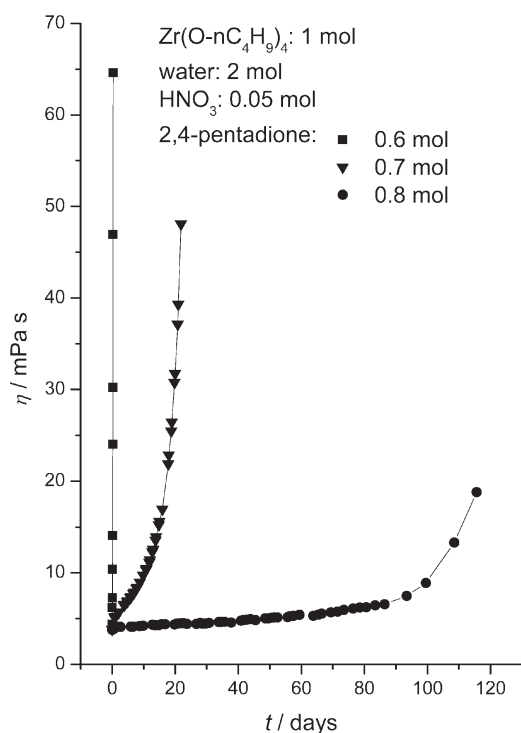


Fig. 1 – Influence of molar ratios of 2,4-pentadione to $\text{Zr}(\text{O}-n\text{C}_4\text{H}_9)_4$ on the rate of viscosity change (gelling rate) of ZrO_2 sols, for molar ratio of acid to $\text{Zr}(\text{O}-n\text{C}_4\text{H}_9)_4$ of 0.05

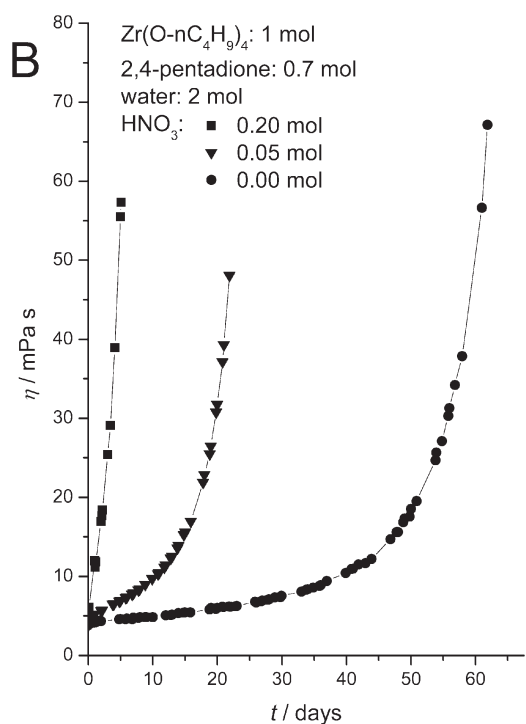
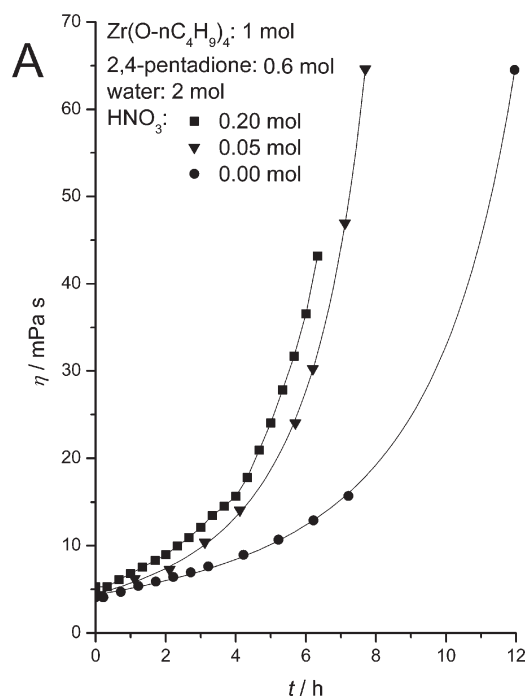


Fig. 2 – Influence of molar ratios of nitric acid to $\text{Zr}(\text{O}-n\text{C}_4\text{H}_9)_4$ on the rate of viscosity change (gelling rate) of ZrO_2 sols, for molar ratio of 2,4-pentadione to $\text{Zr}(\text{O}-n\text{C}_4\text{H}_9)_4$ of 0.6 (A) and 0.7 (B)

For ratio of 0.5, the sol gels immediately, and is thus unsuitable for coating, while for the ratios of 0.6 or greater it is possible to prepare a whole palette of ZrO_2 sols of varying stability, which will in the end form transparent gels. Depending on the molar ratio of 2,4-pentadione, $\text{Zr}(\text{O}-n\text{C}_4\text{H}_9)_4$ can be partially or fully complexed.^{17,19} Complexed $\text{Zr}(\text{O}-n\text{C}_4\text{H}_9)_4$ hy-

hydrolyses more slowly due to the steric interference of the large 2,4-pentadione molecule,²⁰ and thus it prevents the uncontrolled precipitation of zirconium hydroxide. When the molar ratio of 2,4-pentadione to $Zr(O-nC_4H_9)_4$ is less than one, both fully and partially complexed forms exist in the sol. As the ratio of 2,4-pentadione decreases, the portion of fully complexed $Zr(O-nC_4H_9)_4$ decreases until its final disappearance at the ratio 0.5, resulting in immediate gelation of the sol. At even lower ratios of 2,4-pentadione there is enough uncomplexed $Zr(O-nC_4H_9)_4$ to cause the precipitation of hydroxide.

The nitric acid acts as a catalyst for the sol-gel process,²¹ and consequently decreases the gelling time of the sols. As can be seen from the Table 1 and Figure 2, the increased concentration of acid has significantly larger influence on gelling time in systems with a larger 2,4-pentadione content. Since the hydrolysis of metal alkoxides in acid conditions is a nucleophilic reaction initiated by protonization, preferential reaction in these conditions is the hydrolysis of $Me(OR)_4$, rather than $Me(OR)_3(OH)$ molecules. Thus complexed $Zr(O-nC_4H_9)_4$ molecules are more susceptible to hydrolysis and gelation in more acid conditions.

It was found that the gelling kinetic of ZrO_2 sols can be described with an empirical model:²²

$$\eta = \eta_0 \left(\frac{1 + k t}{1 - t/t^*} \right)^a \quad (3)$$

where η_0 is the initial viscosity of the sol, k the rate coefficient, a an empirical exponent and t^* the gelling time. The gelling time is defined as the time required to reach infinitely high viscosity. The kinetic parameters are given in Table 3, and it can be seen that the gelling time acquired by modelling corre-

Table 3 – The gelling parameters from the empirical kinetic model (3)

Sol No.	$k/10^{-3} \text{ h}^{-1}$	a	t^*/h
4			17
5	46.6	1.678	11
6			10
7	1.12		1540
8	6.08	0.670	580
9	82.6		165
10	0.278		4220
11	0.0821	0.440	2860
12	402		155

sponds well with the empirical values given in Table 1. Hence it can be concluded that this model is suitable for description of ZrO_2 sols gelling kinetics.

Crystallisation of gels

To study the crystallisation behaviour of gelled sols, the sol no. 5 in Table 1 was chosen. The results of DSC/TGA analysis are shown in Figure 3. The first endothermic peak at 358 K is linked with the evaporation of residual water and organic solvents. The intense exothermic peaks at 537 K and 606 K, accompanied with large mass loss of 24.2 %, indicate the breaking of the gel structure and the combustion of liberated organic compounds. The exothermic peak at 763 K corresponds to crystallization of tetragonal zirconia. Final exothermic peak, at 827 K, accompanied by minor mass loss (1.7 %) is attributed to the combustion of residual carbon, created by incomplete combustion of organic component in gel.²³ The continued mass loss above 1173 K confirms that the complete combustion of organic components is impossible at lower temperatures. According to these results, 673 K was chosen as the lowest calcination temperature for the coatings.

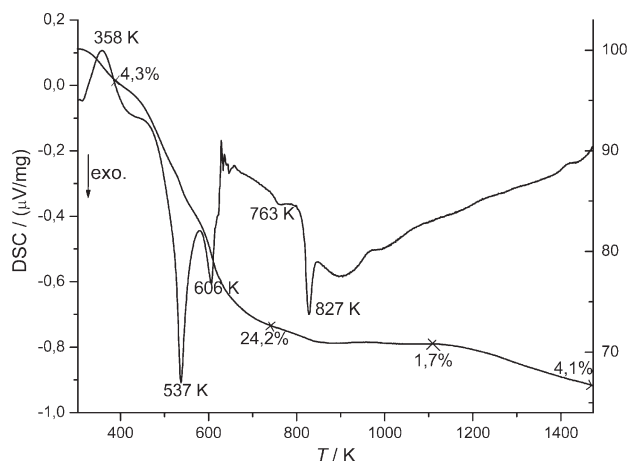


Fig. 3 – DSC/TGA curves of ZrO_2 gel (obtained from the sol no. 5) dried at 378 K

As the mechanical properties of tetragonal zirconia are superior to monoclinic,^{13–15} the influence of firing temperature on phase composition of zirconia was investigated. Figure 4 shows the diffractograms of zirconia powder after firing at listed temperatures. It can be seen that zirconia powder crystallises already at 673 K. It is impossible to confirm whether it is tetragonal or cubic zirconia, or their mixture, since both forms give almost identical diffractograms. But according to the literature,^{24,25} for yttria concentration of 3 % the pure

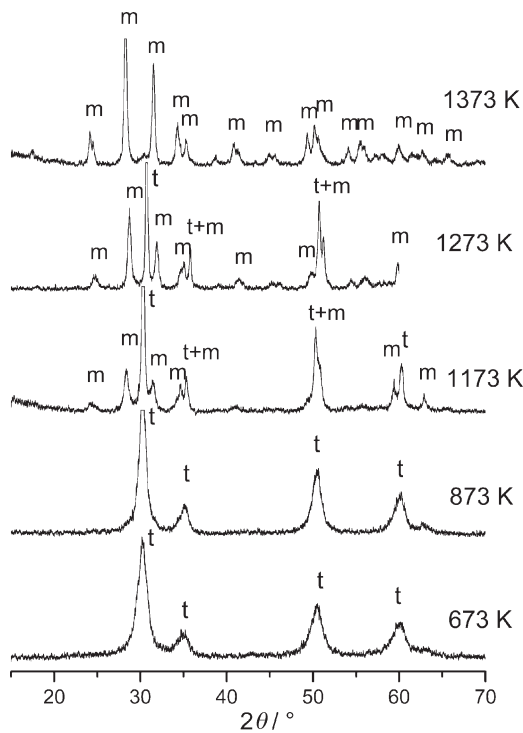


Fig. 4 – XRD Diffractograms of ZrO_2 powder (based on the sol no. 5) fired for 2 hours at listed temperatures (m – monoclinic zirconia, t – tetragonal zirconia)

tetragonal zirconia, $t-ZrO_2$, is regularly stabilised. With increasing firing temperature, the intensities of diffraction maxima, especially (111) maximum, increase. Only at 1173 K do the diffraction maxima of monoclinic phase, $m-ZrO_2$, appear, and the transformation of $t-ZrO_2$ into $m-ZrO_2$ begins. Further temperature increase furthers the transformation, until at 1373 K practically only monoclinic zirconia remains.

Morphology and tribologic properties of zirconia coatings

Figure 5. shows the morphology of the coated surfaces of the samples obtained with the fresh sol no. 8 (Table 1) after firing at 673 K, 873 K and 973 K. It can be seen that the dimension of zirconia grains increases with the firing temperature. Influence of firing temperature and sol viscosity on the microhardness of the coating-substrate system is shown in Figure 6. To determine the abrasion resistance of the coated substrates, the average width of their wear trace was compared with the width of the abrasion wear trace of the substrate, as shown in Figure 7, where the full line represents the width of the abrasion wear trace of the substrate. The increase of microhardness and abrasion resistance with the firing temperature is due to the improved mechanical properties of more completely crystallized zirconia, while the increased sol viscosity re-

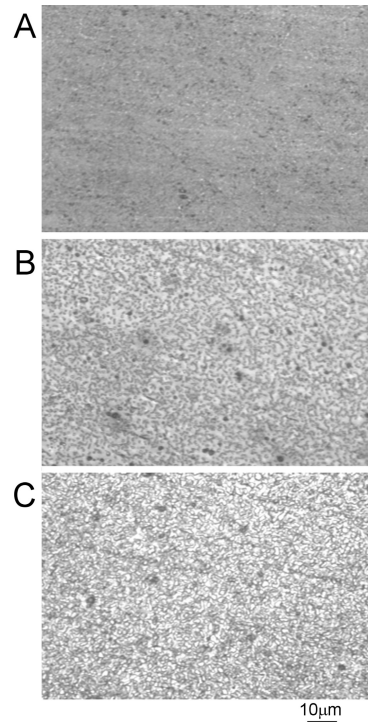


Fig. 5 – Surface morphology of zirconia coating obtained from fresh sol no.8 fired at 673 K (A), 873 K (B) and 973 K (C) for 2 h

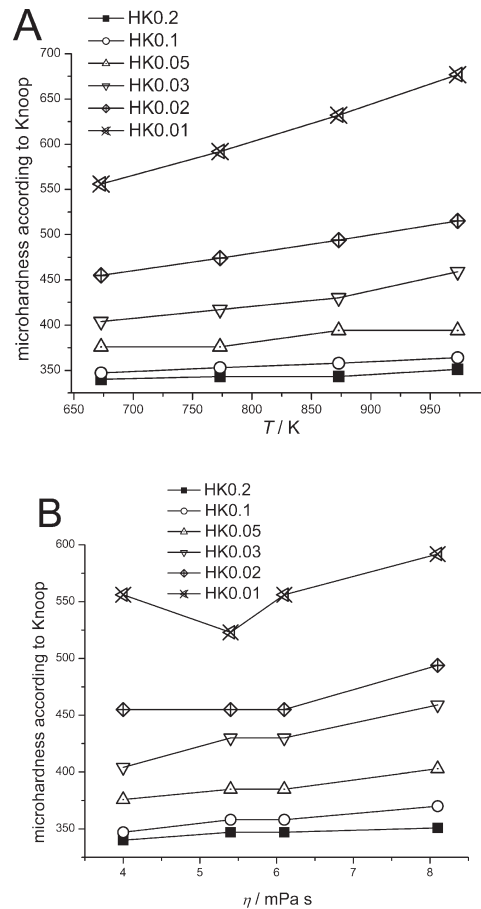


Fig. 6 – Influence of firing temperature (A) and sol viscosity (B) on the microhardness of the coating-substrate system

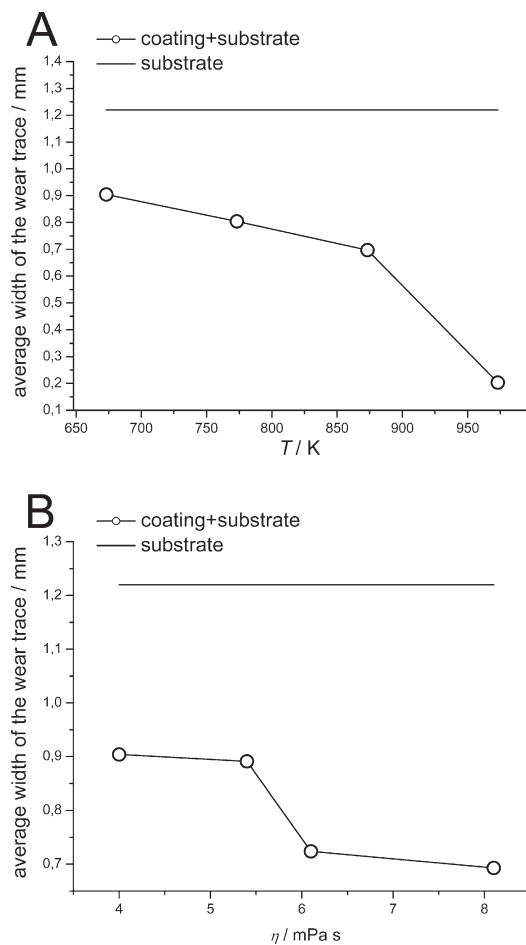


Fig. 7 – Influence of firing temperature (A) and sol viscosity (B) on the abrasion resistance of the coating-substrate system

sults in thicker coatings,²⁶ and therefore also improved mechanical properties. In both cases, the increase of microhardness is more pronounced for decreased test forces, since the influence of the coating on the microhardness of coating-substrate system increases. It can be concluded that the degree of crystallization and the coating thickness both influence the final properties of sol-gel derived zirconia coatings, and further research is planned to optimise the quality and performance of these coatings.

Conclusions

It has been determined that the stability of ZrO_2 sols, and hence their applicability for preparation of thin ceramic coatings, depends on the combined influence of 2,4-pentadione, water and nitric acid, which determine the rates of hydrolysis and condensation of $Zr(O-nC_4H_9)_4$. It was found that tetragonal zirconia crystallizes at 673 K and remains stable up until ~ 1173 K. The grain dimension of zirconia coatings increases with the firing

temperature, and both the firing temperature and sol viscosity influence the final mechanical properties of the coatings.

ACKNOWLEDGEMENTS

The authors would like to thank the Ministry of Education, Science and Sport of the Republic of Croatia for the support.

List of symbols

- a – empirical constant, eq (3)
- d – length of the longest diagonal of the indentation (in Knoop test), mm
- F – force, N
- HK – Knoop hardness, $N\ mm^{-2}$
- k – coefficient of the rate of viscosity change, h^{-1}
- n – amount of substance, mol
- r – molar ratio, n/n
- t – time, h
- t^* – gelling time, h
- T – thermodynamic temperature, K
- β – rate of temperature change, $K\ min^{-1}$
- η – dynamic viscosity, mPa s
- η_0 – initial dynamic viscosity of sols, mPa s

References

1. Atik, M., Aegerter, M. A., *J. Non-Cryst. Solids* **147/148** (1992) 813.
2. Izumi, K., Murakami, M., Deguchi, T., Morita, A., Tohge, N., Minami, T., *J. Am. Ceram. Soc.* **72** (1989) 1465.
3. Di Maggio, R., Scardi, P., Tomasi, A., *Mater. Res. Soc. Symp. Proc.* **180** (1990) 344.
4. Shane, M., Mecartney, M. L., *J. Mater. Sci.* **25** (1990) 1537.
5. Atik, M., Zarzycki, J., R'Kha, C., *J. Mater. Sci. Letters* **13** (1994) 266.
6. Di Maggio, R., Fedrizzi, L., Rossi, S., Scardi, P., *Thin Solid Films* **286** (1996) 127.
7. Li, J. F., Liao, H., Wang, X. Y., Normand, B., Ji, V., Ding, C.X., Coddet, C., *Tribol. Int.* **37** (2004) 77.
8. Espitia-Cabrera, I., Orozo-Hernandez, H., Torres-Sanchez, R., Contreras-Garcia, M.E., Bartolo-Perez, P., Martinez, L., *Mater. Lett.* **58** (2004) 191.
9. Chen, H., Ding, C. X., Zhang, P. Y., La, P. Q., Lee, S. W., *Surf. Coat. Technol.* **173** (2003) 144.
10. Chen, H. A., Zhang, Y. F., Ding, C. X., *Wear* **253** (2002) 885.
11. Štefanić, I., Musić, S., Štefanić, G., Gajović, A., *J. Mol. Structure* **480/481** (1999) 621.
12. Liu, W. M., Chen, Y. X., Ye, C. F., Zhang, P. Y., *Ceram. Internat.* **28** (2002) 349.
13. Fischer, T. E., Anderson, M. P., Jahanmir, S., *J. Am. Ceram. Soc.* **72** (1989) 252.
14. Fischer, T. E., Anderson, M. P., Jahanmir, S., Salher, R., *Wear* **124** (1988) 133.

15. *Zum Gahr, K.-H., Bundschuh, W., Zimmerlin, B., Wear* **162–164** (1993) 269.
16. *Yamada, K., Chow, T. Y., Horihata, T., Nagata, M., J. Non-Cryst. Solids* **100** (1988) 316.
17. Pope, E. J. A., MacKenzie, J. D., *J. Non-Cryst. Solids* **87** (1986) 185.
18. ISO 4545, Metallic materials-Hardness test-Knoop test, 1993.
19. *Bradley, D. C., Carter, D. G., Canad. J. Chem.* **39** (1962) 15.
20. *Debsikdar, J. C., J. Non-Cryst. Solids* **86** (1986) 231.
21. *Yasumori, A., Anma, M., Yamane, Y., Phys. Chem. Glasses* **30** (1989) 193.
22. *Halley, P. J., Mackay, M. E., Polym. Eng. Sci.* **36** (1996) 593.
23. *Rinn, G., Schmidt, H., Am. Ceram. Soc. Ceram. Trans.* **1/A** (1988) 23.
24. *Matsui, M., Soma, T., Oda, J., in Claussen, N., Rühle, M. and Heuer, A.H. (Ed.), Advances in Ceramics Vol. 12, The American Ceramic Society, Columbus, Ohio, 1983, pp. 352–370.*
25. *Schubert, H., Petzow, G., in Claussen, N., Rühle, M. and Heuer, A.H. (Ed.), Advances in Ceramics Vol. 24, The American Ceramic Society, Columbus, Ohio, 1988, pp. 21–28.*
26. *Sakka, S., Yoko, T., Sol-Gel-Derived Coating Films and Applications, in Reifeld, R. and Jørgensen, C.K. (Ed.), Chemistry, Spectroscopy and Applications of Sol-Gel Glasses, Springer-Verlag, Berlin – Heidelberg, 1992, pp. 89–118.*